

See discussions, stats, and author profiles for this publication at: <https://www.researchgate.net/publication/231650010>

# Particle-Size-Dependent Hydrophilicity of TiO<sub>2</sub> Nanoparticles Characterized by Marcus Reorganization Energy of Interfacial Charge Recombination

ARTICLE in THE JOURNAL OF PHYSICAL CHEMISTRY C · MAY 2008

Impact Factor: 4.77 · DOI: 10.1021/jp802532w

---

CITATIONS

10

---

READS

9

3 AUTHORS, INCLUDING:



Yu-Xiang Weng

Chinese Academy of Sciences

45 PUBLICATIONS 781 CITATIONS

SEE PROFILE

# Particle-Size-Dependent Hydrophilicity of TiO<sub>2</sub> Nanoparticles Characterized by Marcus Reorganization Energy of Interfacial Charge Recombination

Ya-Qiong Hao, Yan-Feng Wang, and Yu-Xiang Weng\*

Laboratory of Soft Matter Physics, Institute of Physics, Chinese Academy of Sciences, Beijing 100080, China, and National Laboratory of Condensed Matter Physics, Beijing 100080, China

Received: February 19, 2008

Size-dependent hydrophilicity of TiO<sub>2</sub> nanoparticles has been investigated by an interface transient molecular probe method. The results show that the reorganization energy for the interfacial charge recombination of the probe molecule can be a specific parameter for characterizing the hydrophilicity of the nanoparticles which is in accordance with the density of the surface hydroxyl group as a parallel parameter. The observed hydrophilicity in terms of either reorganization energy or the density of the surface hydroxyl group decays monoexponential with the mean particle diameter, having decay constant of 1/3.2 nm<sup>-1</sup> for the former and 1/1.8 nm<sup>-1</sup> for the latter.

## Introduction

Wide-gap metal-oxide semiconductor nanoparticles have attracted intense interest, because of their size-dependent photophysical properties and chemical activities.<sup>1,2</sup> Among the various types of metal oxides, titania (TiO<sub>2</sub>) is one of the most promising materials in many applications, e.g., quantum dot devices,<sup>3</sup> photocatalysis,<sup>4</sup> and solar energy conversion devices.<sup>5</sup> As a typical semiconductor, excitation of TiO<sub>2</sub> with photon energy higher than its band gap gives rise to excited-state electrons and holes at the conduction and valence bands, respectively, which can initiate various redox reactions at the semiconductor surface or interface. The strong oxidizing power of the photogenerated holes, the chemical inertness, and the nontoxicity of TiO<sub>2</sub> have made it a superior photocatalyst.<sup>4,6</sup>

An intriguing property of TiO<sub>2</sub> is its switch between the hydrophobic and hydrophilic state upon UV light irradiation.<sup>7,8</sup> Although a TiO<sub>2</sub> surface is originally less hydrophilic, it becomes highly hydrophilic by its band gap excitation via UV light irradiation and gradually reverts to originally less hydrophilic in the dark. The unique amphiphilic surface character has been achieved on both single crystals and polycrystalline thin films coated on various substrates, e.g., glass, ceramics, plastics, metals, and polymer films. The mechanism of UV light-induced hydrophilic/hydrophobic conversion has been studied intensively.<sup>9–11</sup> However, such a conversion has only been observed for a large single crystal or film samples which are suitable for water contact angle measurement. As the size of the crystal gets smaller, the surface area of the particle increases drastically, giving rise to undercoordination of the surface Ti atoms, namely 5-fold and 4-fold coordinated,<sup>12,13</sup> which is expected to result in a size-dependent hydrophilicity. Nonetheless, characterizing the hydrophilicity of particles with size at nanoscale is a challenging task due to lack of a proper method as well as a proper parameter such as “contact angle of water” used for large size.

We have developed a transient molecular probe method previously<sup>13–17</sup> which is sensitive only to the adsorbed

monolayer at the TiO<sub>2</sub> surface. The probe molecule is all-*trans*-retinoic acid (ATRA); it can be attached onto the TiO<sub>2</sub> surface by formation of a chemical bond between the carboxylic group and the surface Ti atoms. After photoexcitation of ATRA, the excited-state of the ATRA molecule would inject an electron into the conduction band of TiO<sub>2</sub>, and the subsequent interfacial charge recombination would generate an excited-triplet-state ATRA (ATRA<sup>T</sup>). We found that the transient ATRA<sup>T</sup> absorption spectrum can be used to probe the various interface properties of TiO<sub>2</sub> nanoparticles including the carboxylic binding forms at the surface, size-dependent coordination number of the surface Ti atoms. Recently we have detected the light-induced hydrophilicity/hydrophobicity conversion of TiO<sub>2</sub> nanoparticles by this transient molecular probe method, in which the reorganization energy change of the photoinduced interfacial charge recombination of the probe molecule was proposed as an indicator for such a conversion process,<sup>16</sup> where the ATRA probe molecule was chemically adsorbed onto TiO<sub>2</sub> nanoparticle (6.0 nm) in an alcoholic solution containing a small amount of water. After photoexcitation by 355 nm laser, the decay kinetics for the interfacial charge recombination generated ATRA<sup>T</sup> was measured, which actually traces the charge recombination to the ground state.<sup>14,17</sup> We have confirmed that the interfacial charge recombination process follows the Marcus equation  $k_{ET} = k_0 \exp[-(\Delta G + \lambda)^2/4\lambda k_B T]$ ,<sup>18</sup> i.e., a plot of  $\ln k_{ET}$  against  $1/T$  would give a linear relationship with a slope of  $-(\Delta G + \lambda)^2/4\lambda k_B$  and an intercept of  $\ln k_0$ , where  $T$  is the absolute temperature,  $\Delta G$  is the free energy difference,  $\lambda$  is the Marcus reorganization energy, and  $k_B$  is the Boltzmann constant. In this way, the photoinduced hydrophilicity/hydrophobicity conversion of the TiO<sub>2</sub> nanoparticle surface due to the local polarity change around the individual nanoparticle was successfully demonstrated in terms of the reorganization energy, i.e., a larger reorganization energy corresponds to a faster charge recombination.<sup>16</sup> Therefore, the reorganization energy for the interfacial charge recombination can be a specific parameter for characterizing the hydrophilicity of TiO<sub>2</sub> nanoparticles. In this work, we quantitatively investigate the effect of the particle size on the hydrophilicity of the TiO<sub>2</sub> nanoparticles by the use of

\* Corresponding author. Tel: 86-10-82648118. Fax: 86-10-82648118. E-mail: yxweng@aphy.iphy.ac.cn.

the proposed method. The result shows that the hydrophilicity of the TiO<sub>2</sub> nanoparticles measured in terms of the reorganization energy decays monoexponential with the particle size.

## Experimental Section

**Materials.** ATRA (Aldrich) and titanium (IV) tetra-isopropoxide (98%) (ACROS) were used as received. Solvents and other reagents were analytical grade and used without further purification. Water was deionized (Milli-Q, Millipore Corp.).

**(a) Preparation of TiO<sub>2</sub> Nanoparticles of Varied Size.** TiO<sub>2</sub> colloidal solutions were prepared by controlled hydrolysis of titanium (IV) tetra-isopropoxide in water under controlled pH. The procedures have been described elsewhere;<sup>13,19</sup> briefly, aqueous TiO<sub>2</sub> colloidal solutions were prepared by a dropwise addition of titanium(IV) tetra-isopropoxide (25 mL) dissolved in 10 mL of 2-propanol into 150 mL of deionized H<sub>2</sub>O at a given acidity adjusted with 68% nitric acid solution cooled by an ice/water bath under vigorous stirring. A white precipitate formed instantaneously. Immediately after the hydrolysis, the slurry was heated to 80 °C and stirred vigorously for 8 h, to achieve peptization. The solution was then filtered on a glass frit to remove nonpeptized agglomerates as well as dust. After sonicated for 1 h, the colloidal suspension was introduced into a rotary evaporator and evaporated at 42 °C to a dried powder of TiO<sub>2</sub>. We found that the size of the nanoparticles depends critically on the amount of HNO<sub>3</sub> added in the solution. By controlling the amount of added HNO<sub>3</sub>, a series of TiO<sub>2</sub> nanoparticles with varied size, i.e., 2.0, 4.1, 4.6, 5.5 and 5.8 nm, were synthesized.

To obtain TiO<sub>2</sub> nanoparticles with a 3.1 nm size, the TiO<sub>2</sub> powder (4.1 nm) was resuspended in H<sub>2</sub>O (pH 3.0) and ultracentrifuged (Hitachi Preparative Ultracentrifuge cp 100MX) at 60 000 rpm for 45 min. Then the solvent of the supernatant was removed by rotary evaporation at 42 °C to obtain the dried TiO<sub>2</sub> powder.

**(b) Dye-Sensitization of TiO<sub>2</sub> Colloidal Solution.** The TiO<sub>2</sub> colloidal solution was prepared by redissolving the dried TiO<sub>2</sub> powder into the mixed solution of methanol and H<sub>2</sub>O whose pH value was preadjusted to 3.0 with nitric acid ( $v_{\text{methanol}}:v_{\text{H}_2\text{O}} = 19:1$ ). The ATRA-sensitized TiO<sub>2</sub> colloidal solution was prepared by addition of the concentrated ATRA methanol solution ( $c = 2 \times 10^{-3}$  M) into the TiO<sub>2</sub> colloidal solution and stirring for 30 min in the dark under high-purity argon gas stream for dye sensitization, keeping the apparent ATRA concentration in the bulk at  $2 \times 10^{-5}$  M. The resulting solution was bubbled with high purity argon gas for at least half an hour to remove the dissolved oxygen.

**Measurements.** The morphology of the as-obtained TiO<sub>2</sub> powders were examined by high-resolution transmission electron microscopy (TEM). The samples were prepared by depositing a small amount of the suspensions onto a carbon-coated copper grid (mesh 200). TEM images were taken on a JEM-2010 (Japan) electron microscope. The flash photolysis setup has been reported elsewhere.<sup>20,21</sup> Briefly, it employed the 355 nm third harmonic generation of a Nd<sup>3+</sup>:YAG laser (Spectra Physics) as the excitation source (Quanta Ray DCR) at the repetition rate of 10 Hz with a pulse width (full-width-at-half-measure) of 8 ns. The probe beam source was a 500 W continuous wave (cw) Xe lamp, and the transient signal was detected by a six-stage R456 (Hamamatsu) photomultiplier tube (PMT), amplified by a 300 MHz DC (Stanford Research Systems, Inc.) amplifier, and the amplified signal

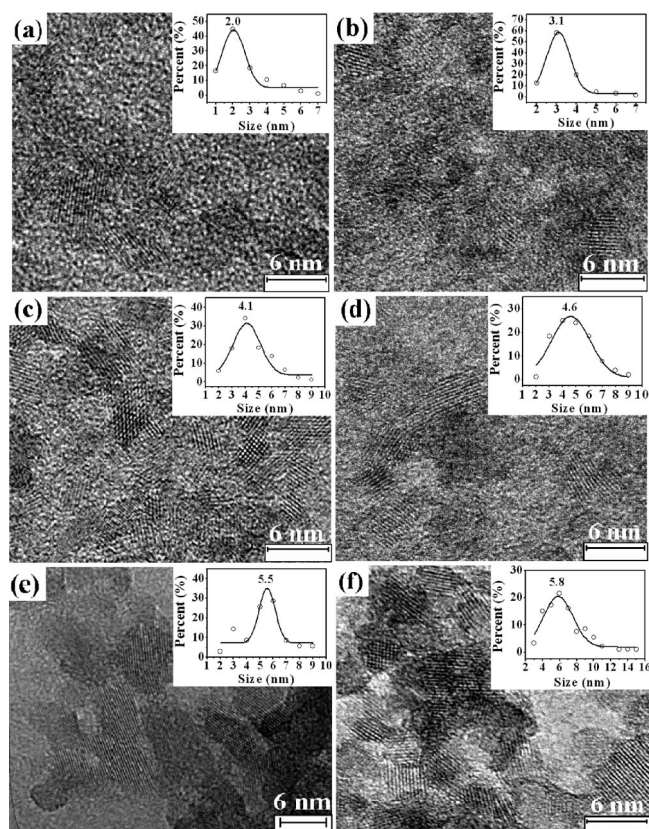


**Figure 1.** TEM images of a series of TiO<sub>2</sub> nanoparticles with varied size: (a) 2.0 nm, (b) 3.1 nm, (c) 4.1 nm, (d) 4.6 nm, (e) 5.5 nm, and (f) 5.8 nm. (Inset) Size distribution of corresponding TiO<sub>2</sub> nanoparticles obtained from the analysis of the corresponding TEM image with Image-Pro Plus software.

was recorded on a 500 MHz digital oscilloscope (Tektronix) interfaced to a personal computer (PC) by a general-purpose interface bus (GPIB) board for data handling and processing. The charge recombination kinetics was probed at 440 nm where the adsorbed ATRA molecule has a maximum triplet-triplet absorption. A narrow band-pass filter centered at 440 nm was used to select the 440 nm probe light. After passing the sample, the probe beam was sent to a monochromator before detection by the PMT. The 355 nm excitation beam was perpendicular with the probe beam. During the experiment, the ATRA-sensitized TiO<sub>2</sub> colloidal solutions were kept bubbling with a high-purity argon gas stream. The charge recombination kinetics was measured at a constant temperature by placing the sample cell into a water jacket circulated by flowing water of a controlled temperature of 25 °C.

## Results and Discussion

Figure 1 shows a series of typical TEM images of TiO<sub>2</sub> of varied sizes along with the plots of the size distribution conducted by Image-Pro Plus analysis software. A statistical analysis of particles in TEM images yielded an average particle diameter. The average particle diameter distributions can be fitted by single-peak Gaussian function, and the resulting average diameters together with the standard deviations are summarized in Table 1.

During the ATRA triplet decay measurement, it has been known that the TiO<sub>2</sub> nanoparticles undergo repeated light-induced hydrophilic-hydrophobic conversion when subjected to prolonged laser irradiation.<sup>16</sup> For characterization of the hydrophilicity of the TiO<sub>2</sub> nanoparticles, it is necessary to find out

**TABLE 1: TEM Evaluated Diameters for TiO<sub>2</sub> Nanoparticles and the Measured Decay Time Constants for ATRA/TiO<sub>2</sub> at the Hydrophilic State**

particle size (nm)	2.0 ± 0.1	3.1 ± 0.1	4.1 ± 0.2	4.6 ± 0.2	5.5 ± 0.1	5.8 ± 0.2
lifetime (μs)	3.0 ± 1.2	4.0 ± 1.6	7.6 ± 1.4	10.8 ± 2.5	16.9 ± 2.7	20.9 ± 3.5

the hydrophilic state which is specific to the nanoparticles of a given size. Therefore, for every sample, prolonged laser irradiation was performed to search the hydrophilic-to-hydrophobic interconversion process, by which the charge recombination time constant at the hydrophilic state can thus be determined. Such a searching process for every sample has been repeated independently at least three times. Figure 2 presents a series of photoinduced hydrophilic/hydrophobic transition curves measured using the ATRA<sup>T</sup> decay time constant against the laser irradiation time for TiO<sub>2</sub> nanoparticles of varied size, in which the hydrophilic region was marked by two solid lines. To obtain the ATRA<sup>T</sup> decay time constant at the given particle size, a number of data points at the hydrophilic state within the marked area for every sample were averaged, the results are listed in Table 1. Applying the Marcus relation with  $\Delta G = -0.8$  eV and  $\ln k_0 = 12.77 \pm 0.27$ ,<sup>16</sup> the reorganization energy  $\lambda$  at the hydrophilic state thus can be determined from the measured charge recombination rate of the

hydrophilic state accordingly. Figure 3 plots  $\lambda$  (open circles) against the size of TiO<sub>2</sub> nanoparticles, which can be fitted by a monoexponential decay equation with a decay constant of  $1/3.2$  nm<sup>-1</sup>. This provides an account for the phenomenon that, when the size of TiO<sub>2</sub> nanoparticles exceeds 6 nm, the particles can hardly be dispersed in water, in remarkable contrast to SiO<sub>2</sub> nanoparticles which can easily be dispersed in water at a much larger size.

The observed phenomenon can be readily understood in terms of the surface trapped electrons. As investigated in our early study,<sup>13</sup> the surface Ti atoms of TiO<sub>2</sub> nanoparticles exist mainly in three forms, i.e., saturated coordination state (6-fold coordinated) and undercoordination state (5-fold or 4-fold coordinated). The relative compositions of the three different types of surface Ti atoms are varied with the size of the nanoparticles. Table 2 summarizes the size-dependent compositions of the surface Ti atoms of different coordination numbers. The electrons trapped at the surface Ti<sup>3+</sup> trapping sites (underco-

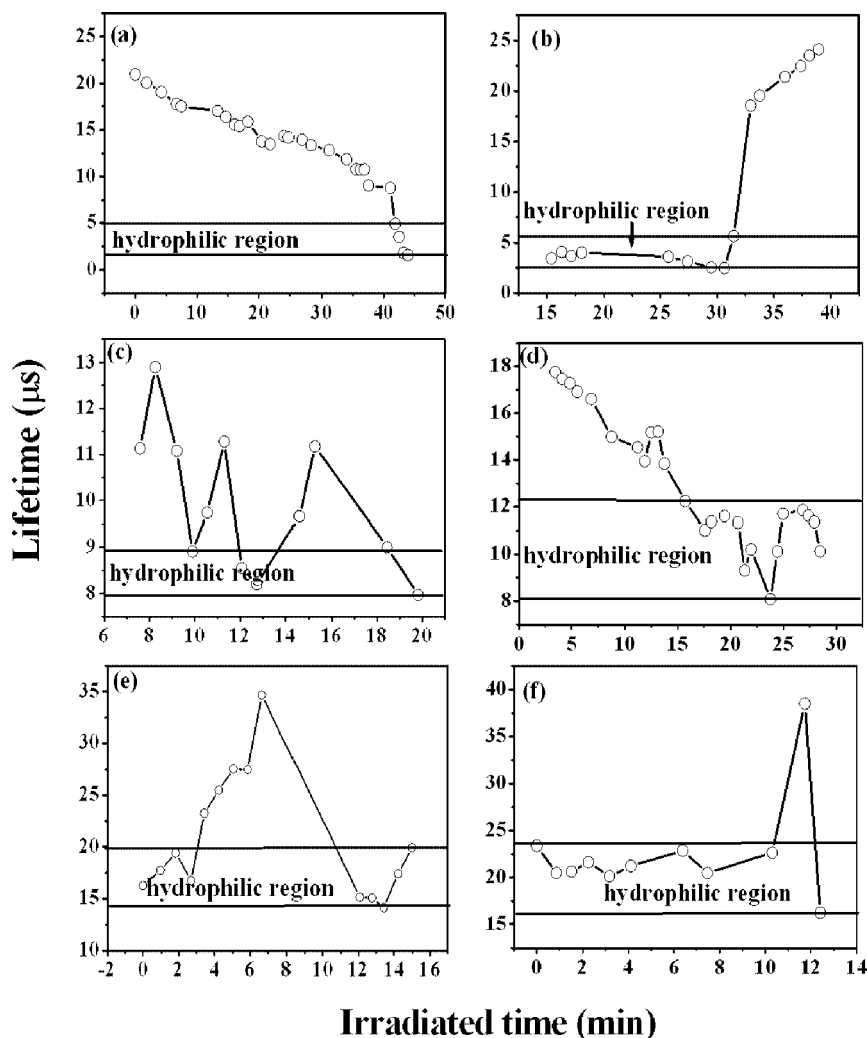


**Figure 2.** Light-induced hydrophilic/hydrophobic interconversion in terms of the interfacial charge recombination decay time constant observed for ATRA ( $c = 2.0 \times 10^{-5}$  M)/TiO<sub>2</sub> of varied sizes: (a) 2.0 nm, (b) 3.1 nm, (c) 4.1 nm, (d) 4.6 nm, (e) 5.5 nm, and (f) 5.8 nm in methanol/H<sub>2</sub>O ( $v_{\text{methanol}}:v_{\text{H}_2\text{O}} = 19:1$ ) solution subjected to prolonged 355 nm laser irradiation at a power of  $0.8$  mJ/(cm<sup>2</sup> pulse) and a repetition rate of 10 Hz, pH 3.0, at 25 °C.



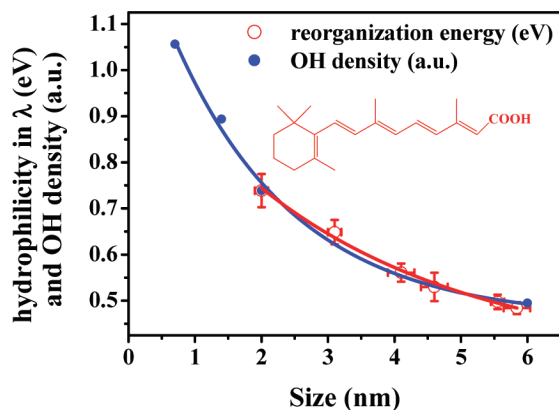


**Figure 3.** Plot of the reorganization energy of ATRA ( $c = 2.0 \times 10^{-5}$  M)/TiO<sub>2</sub> (2.0 g/L) in methanol/H<sub>2</sub>O (v:v 19:1) (○) and relative surface OH density (●) against the size of TiO<sub>2</sub> nanoparticles. Solid lines are monoexponential fitting curves. The graphic inset is the molecular structure of ATRA.

**TABLE 2: Compositions of the Three Different Surface Ti Atoms for TiO<sub>2</sub> Nanoparticles of Varied Size**

size (nm)	composition (%)			relative density of the surface OH group
	6-fold	5-fold	4-fold	
0.7 <sup>13</sup>	0	57	43	143
1.4 <sup>13</sup>	0	79	21	121
2.0 <sup>22</sup>	0	100	0	100
6.0 <sup>13</sup>	33	67	0	67

ordinated) preferentially adsorb the dissociative water, increasing the microenvironmental hydrophilicity surrounding the TiO<sub>2</sub> nanoparticle by generating more surface hydroxyl groups, giving rise to a more polar local environment around the nanoparticle and a larger reorganization energy. Therefore when reducing the nanoparticle size, the density of the surface hydroxyl groups would increase dramatically, this can lead to a substantial increase in the reorganization energy hence the hydrophilicity of the nanoparticles (see Table 2).

The density of the surface hydroxyl group can also be a parameter for characterizing the hydrophilicity of the TiO<sub>2</sub> nanoparticles.<sup>7,12,23–25</sup> Fujishima et al. have found the photogeneration of an amphoteric TiO<sub>2</sub> surface by friction force microscopic (FFM) and X-ray photoelectron spectroscopy. They illustrated that ultraviolet irradiation may create surface oxygen vacancies at bridging sites, resulting in the conversion of relevant Ti<sup>4+</sup> sites to Ti<sup>3+</sup> sites which are favorable for dissociative water adsorption. These defects presumably influence the affinity for chemisorbed water for their surrounding five-coordinated Ti sites and thereby result in the formation of hydrophilic domains, leaving the remainder oleophilic. On long-term storage in the dark, the chemisorbed hydroxyl groups are replaced with oxygen from the air.<sup>7,23</sup> Meanwhile, they also have investigated the hydrophilic/hydrophobic conversion of the surface of the TiO<sub>2</sub> film by Fourier transform infrared (FTIR) spectroscopy. IR bands attributed to the hydroxyl group and molecular water that are positioned at 3695, 3300, and 1623 cm<sup>-1</sup> were all observed. This result indicates the coexistence of dissociated and molecular water on the TiO<sub>2</sub> surface. With UV illumination, the enhancement in the amount of adsorbed dissociated water and a reduction of the amount of adsorbed molecular water has been verified. Storage in the dark resulted in the decrease of all of the bands, correlated with both hydroxyl desorption at the defect sites and the desorption of molecular water.<sup>12</sup> Premkumar has achieved the hydrophilic/hydrophobic conversions on the TiO<sub>2</sub> surface by applying high anodic oxidation potentials. The X-ray

photoemission spectrum (XPS) showed the increase in the surface hydroxyl group and the decrease in the surface carbon content on the surface of the potential-induced superhydrophilic TiO<sub>2</sub>.<sup>24</sup> Shultz et al. have investigated the molecular species adsorbed on the surface of nanoparticulate anatase TiO<sub>2</sub> films by visible-infrared sum frequency generation (SFG). An enhanced SFG signal of surface hydroxyl groups on TiO<sub>2</sub> after UV light irradiation has been observed, which confirms that the hydrophilicity is caused by a photoinduced increase in the surface hydroxyl groups.<sup>25</sup> On the basis of these observations, water molecules are dissociatively coordinated to the surface coordination-unsaturated Ti to form surface hydroxyl groups. It is expected that the number of hydroxyl groups formed at the 6-fold Ti surface atom is 0, 5-fold is 1, and 4-fold is 2. Therefore, the relative density of the surface hydroxyl group on TiO<sub>2</sub> surface of different size can be calculated from sum of the composition for different type of surface Ti atoms weighted by the number of the hydroxyl groups they can form by dissociative adsorption of water molecules. Figure 3 plots the relative density of hydroxyl group (solid circles) against the TiO<sub>2</sub> nanoparticle size, which is linearly scaled to that of the size-dependent free energy by setting the value of the former equal to that of the latter at the size of 2.0 nm for better comparison and is fitted by a monoexponential decay equation with a decay constant of 1/1.8 nm<sup>-1</sup>. Apparently these two curves match well with each other, which indicates that both the reorganization energy for the interfacial charge recombination and the relative density of the surface hydroxyl group describe the same size-dependent hydrophilicity of TiO<sub>2</sub> nanoparticles. Therefore, the density of the surface hydroxyl groups reveals the true nature of the size-dependent hydrophilicity for the TiO<sub>2</sub> nanoparticles as shown schematically in Figure 4, and we believe that such a concept can be readily used in characterizing the size-dependent hydrophilicity of nanocrystalline of other oxide materials.

In the current system, we have used water and methanol as the mixed solvent and the transient molecular probe can successfully report the size-dependent hydrophilicity of the TiO<sub>2</sub> nanoparticle in terms of reorganization energy as well as the density of the surface hydroxyl group. However, the experiment does not justify itself whether the reorganization energy change is caused by the surface-hydrophilicity induced local polarity change or simply due to the effect of the size change of a charged nanoparticle as noticed by one of the reviewers. Based on Marcus two-sphere dielectric continuum model, the reorganization energy due to the solvent polarity can be described by  $\lambda_s = (\Delta q)^2 \left( \frac{1}{2r_D} + \frac{1}{2r_A} - \frac{1}{r_{DA}} \right) \left( \frac{1}{\epsilon_\infty} - \frac{1}{\epsilon_0} \right)$ , where the Pekar factor  $\frac{1}{\epsilon_\infty} - \frac{1}{\epsilon_0}$  is approximately the same for water (0.543) and methanol (0.538), which predicts 0.92% reduction in the reorganization energy going from pure water to methanol. To illustrate the mixed solvent effect on the reorganization energy, we have conducted the experiment of measuring the reorganization energy against the molar fraction of methanol by determination of the ATRA<sup>†</sup> decay time constant when adsorbed onto TiO<sub>2</sub> nanoparticles with an average diameter of 6 nm, and the result is shown in Figure 5. Since ATRA can not be dissolved in pure water, and we started at a methanol mole fraction of 26% and ended at a value of 87%, it can be found that the reorganization energy drops by 11.3% even between this intermediate region, already about 11 times the expected value. Obviously the two-sphere dielectric continuum model proposed for a single solvent is no longer valid for the mixed solvent of water and methanol, for the property of this mixed solvent can be very different from its individual

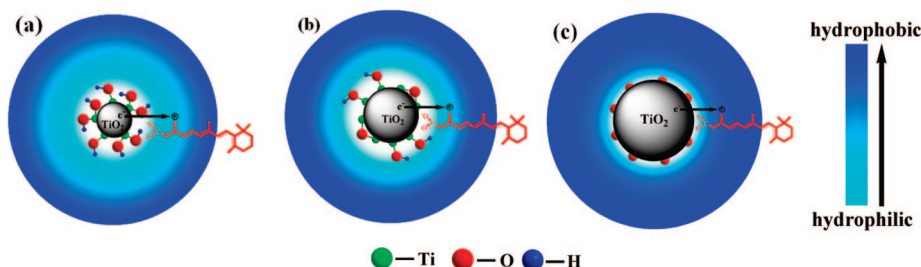


**Figure 4.** Schematic diagram showing the size-dependence hydrophobicity of the TiO<sub>2</sub> nanoparticle detected by the ATRA molecular probe. The hydrophobicity is increased from cyan to blue.

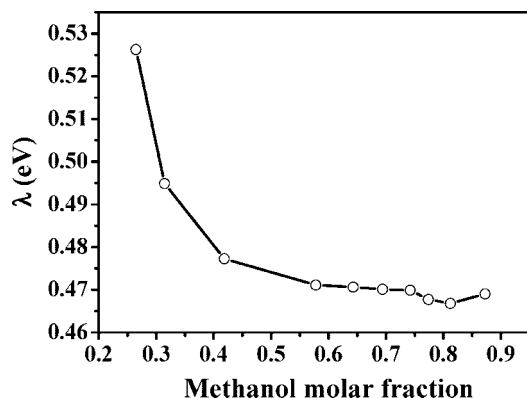


**Figure 5.** Plot of the reorganization energy against the methanol fraction in ATRA/TiO<sub>2</sub> (6 nm) methanol/H<sub>2</sub>O. Excitation power: 1 mJ/(cm<sup>2</sup> pulse).

component alone. Zhang et al. reported that water and methanol alone are good solvents for poly(*N*-isopropylacrylamide) but not certain fractions of their mixture, especially when the methanol content lies in the mole fraction region of 17–47%.<sup>26</sup> They ascribed this fact to the formation of the water/methanol complex chain in the mixed solvent. When the methanol mole fraction is in the range of 17–50%, there is no free water molecules due to formation of the complex (H<sub>2</sub>O)<sub>*m*</sub>(CH<sub>3</sub>OH)<sub>*n*</sub>, where *m/n* varies from 5 to 1, indicating the that water pentamer picks up a methanol molecule from 1 up to 5 depending on the mole fraction of the methanol added, and the polarity of the water/methanol drops drastically with respect to water and methanol alone. Our observed drastic drop of the reorganization energy ends around 42%, in agreement with the observed phenomenon of Zhang et al. However, Figure 5 clearly reveals that the reorganization energies in water and in methanol are different even though their Pekar factors are similar. This can be ascribed to the fact that, at the TiO<sub>2</sub> interface, the water molecules (which are always present at the surface) form the dissociative adsorbed layer first, then come to the hydrogen bonding layers, and finally to the free water molecule layers. This layered structure for the solvent molecules is obviously different from the dielectric continuum model where the solvent molecules are randomly orientated.

On the other hand, we can hardly ascribe the size-dependent reorganization energy change to the size change of the charged particle, which can be described by Born formula,<sup>27,28</sup> i.e.,  $\lambda_s = \{1/2\}(1 - \{1/\epsilon_s\})\{\Delta q^2/r_0\}$ , where *r*<sub>0</sub> is the radius of the nanoparticles and  $\epsilon_s$  is the static dielectric constant. Since a femtosecond time-resolved spectroscopic study of the interfacial charge recombination kinetics have shown that the charge of the injected electron is not evenly distributed on the entire TiO<sub>2</sub> surface but would rather be trapped at a limited local region about 1–2 nm in diameter around the oxidized adsorbed dye molecule regardless of the

particle size,<sup>15,29,30</sup> that is, for TiO<sub>2</sub> particles of different sizes, their contribution of charge to the reorganization energy would be the same. Therefore, we concluded that the observed reorganization energy change versus varied TiO<sub>2</sub> particle size is due to the surface-hydrophilicity induced local polarity change of the mixed solvent.

## Conclusions

We have demonstrated that TiO<sub>2</sub> nanoparticles have a size-dependent hydrophilicity. Both the reorganization energy of the interfacial charge recombination and the density of the surface hydroxyl group can serve as a quantitative parameter for the hydrophilicity of the TiO<sub>2</sub> nanoparticles. Especially, experimental determination of the reorganization energy of the interfacial charge recombination can be a practical method for evaluating the hydrophilicity of nanoparticles other than TiO<sub>2</sub>.

**Acknowledgment.** We thank Prof. Xiangyuan Li for helpful discussion on the reorganization energy in the mixed solvent and bringing ref 26 to our attention. This research has been supported by the Chinese Academy of Sciences innovative Project KJCX2-SW-w29 and the NSFC program under Grant Nos. 60321002 and 20703062.

## References and Notes

- Alivisatos, A. P. *Science* **1996**, 271, 933.
- Sclafani, A.; Palmisano, L.; Schiavello, M. *J. Phys. Chem.* **1990**, 94, 829.
- Colvin, V. L.; Schlamp, M. C.; Alivisatos, A. P. *Nature* **1994**, 370, 354.
- Linsebigler, A. L.; Lu, G.; Yates, J. T., Jr. *Chem. Rev.* **1995**, 95, 735.
- Hagfeldt, A.; Grätzel, M. *Chem. Rev.* **1995**, 95, 49.
- Fox, M. A.; Dulay, M. T. *Chem. Rev.* **1993**, 93, 341.
- Wang, R.; Hashimoto, K.; Fujishima, A.; Chikuni, M.; Kojima, E.; Kitamura, A.; Shimohigoshi, M.; Watanabe, T. *Nature* **1997**, 388, 431.
- Sakai, N.; Fujishima, A.; Watanabe, T.; Hashimoto, K. *J. Phys. Chem. B* **2003**, 107, 1028.
- Feng, X.; Zhai, J.; Jiang, L. *Angew. Chem., Int. Ed.* **2005**, 44, 5115.
- Zhang, X.; Jin, M.; Liu, Z.; Tryk, D. A.; Nishimoto, S.; Murakami, T.; Fujishima, A. *J. Phys. Chem. C* **2007**, 111, 14521.
- Zhang, X.; Jin, M.; Liu, Z.; Nishimoto, S.; Saito, H.; Murakami, T.; Fujishima, A. *Langmuir* **2006**, 22, 9477.
- Wang, R.; Hashimoto, K.; Fujishima, A.; Chikuni, M.; Kojima, E.; Kitamura, A.; Shimohigoshi, M.; Watanabe, T. *Adv. Mater.* **1998**, 10, 135.
- Zhang, Q.-L.; Du, L.-C.; Weng, Y.-X.; Wang, L.; Chen, H.-Y.; Li, J.-Q. *J. Phys. Chem. B* **2004**, 108, 15077.
- Weng, Y.-X.; Li, L.; Liu, Y.; Wang, L.; Yang, G.-Z.; Sheng, J.-Q. *Chem. Phys. Lett.* **2002**, 355, 294.
- Zhang, L.; Yang, J.; Wang, L.; Yang, G.-Z.; Weng, Y.-X. *J. Phys. Chem. B* **2003**, 107, 13688.
- Du, L.-C.; Weng, Y.-X. *J. Phys. Chem. C* **2007**, 111, 4567.
- Weng, Y.-X.; Li, L.; Liu, Y.; Wang, L.; Yang, G.-Z. *J. Phys. Chem. B* **2003**, 107, 4356.
- Marcus, R. A.; Sutin, N. *Biochim. Biophys. Acta* **1985**, 811, 265.

- (19) Papageorgiou, N.; Barbé, C.; Grätzel, M. *J. Phys. Chem. B* **1998**, *102*, 4156.
- (20) Weng, Y.-X.; Chan, K.-C.; Zheng, B.-C.; Che, C.-M. *J. Chem. Phys.* **1998**, *109*, 5948.
- (21) Weng, Y.-X.; Xiao, H.; Chan, K.-C.; Che, C.-M. *J. Phys. Chem. B* **2000**, *104*, 7713.
- (22) Rajh, T.; Nedeljkovic, J. M.; Chen, L. X.; Poluektov, O.; Thurnauer, M. C. *J. Phys. Chem. B* **1999**, *103*, 3515.
- (23) Sakai, N.; Wang, R.; Fujishima, A.; Watanabe, T.; Hashimoto, K. *Langmuir* **1998**, *14*, 5918.
- (24) Premkumar, J. *Chem. Mater.* **2005**, *17*, 944.
- (25) Wang, C.-y.; Groenzin, H.; Schultz, M. J. *Langmuir* **2003**, *19*, 7330.
- (26) Zhang, G.; Wu, C. *J. Am. Chem. Soc.* **2001**, *123*, 1376.
- (27) Rashin, A. A.; Honig, B. *J. Phys. Chem.* **1985**, *89*, 5588.
- (28) Born, M. Z. *Phys.* **1920**, *1*, 45.
- (29) Martini, I.; Hodak, J. H.; Hartland, G. *J. Phys. Chem. B* **1999**, *103*, 9104.
- (30) Weng, Y.-X.; Wang, Y.-Q.; Asbury, J. B.; Ghosh, H. N.; Lian, T. *J. Phys. Chem. B* **2000**, *104*, 93.

JP802532W